Techno-economical Model based Optimal Sizing of PV-Battery Systems for Microgrids

Bandyopadhyay, S; Mouli, GR Chandra; Qin, Zian; Elizondo, L Ramirez; Bauer, Pavol

DOI
10.1109/TSTE.2019.2936129

Publication date
2019

Document Version
Final published version

Published in
IEEE Transactions on Sustainable Energy

Techno-Economical Model Based Optimal Sizing of PV-Battery Systems for Microgrids

Soumya Bandyopadhyay, *Student Member, IEEE*, Gautham Ram Chandra Mouli, *Member, IEEE*, Zian Qin, *Member, IEEE*, Laura Ramirez Elizondo, *Member, IEEE*, and Pavol Bauer, *Senior Member, IEEE*

***Abstract*—Microgrid with integrated photo-voltaics (PV) and battery storage system (BSS) is a promising technology for future residential applications. Optimally sizing the PV system and BSS can maximise self-sufficiency, grid relief, and at the same time can be cost-effective by exploiting tariff incentives. To that end, this paper presents a comprehensive optimisation model for the sizing of PV, battery, and grid converter for a microgrid system considering multiple objectives like energy autonomy, power autonomy, payback period, and capital costs. The proposed approach involves developing a holistic techno-economic microgrid model based on variables like PV system power, azimuth angle, battery size, converter ratings, capital investment and electricity tariffs. The proposed method is applied to determine the optimum capacity of a PV system and BSS for two case residential load profiles in the Netherlands and Texas, US to investigate the effect of meteorological conditions on the relative size of PV and battery. Based on the optimisation results, thumb rules for optimal system sizing are derived to facilitate microgrid design engineers during the initial design phase.**

***Index Terms*—Batteries, microgrids, optimal sizing, particle swarm optimisation, renewable energy, techno-economical analysis.**

I. Introduction

INCREASING energy consumption of buildings (both residential and commercial) has led to 40% of total energy consumption in developed countries [1]. The rise of energy demand in buildings will continue in the near future because of population growth, urbanisation, increasing penetration of electric vehicles (EVs) [2], and electrification of household heating [3], [4]. To solve these problems, "Microgrid" based future electrical power systems have been proposed. A microgrid is a low voltage (LV) power network containing distributed energy sources such as photovoltaic (PV) arrays, micro-wind turbines, fuel cell and energy storage devices [5]. Additionally, energy efficiency of the Microgrid can be improved by choosing direct current (dc) distribution instead of conventional ac based distribution [6]–[9].

Several publications have proposed optimal sizing of PV-battery systems by maximising the economic value created by using battery and PV system focusing on improving self-consumption or energy autonomy [10], [11]. Other studies have focused on optimal sizing of only the battery with the goal of maximising peak-shaving [12]–[14]. A MILP based optimisation model for system sizing for grid-connected and off-grid microgrids is presented in [15]–[17].

However, there are several limitations in current literature regarding the optimal sizing of PV-battery systems for microgrids. First, most studies focus on a single objective like increasing self-consumption, or reduce demand peaks or maximise economic benefits [13], [15], [16]. Due to the mutually conflicting nature of the targets, the single objective optimisation approach is unable to provide valuable insights regarding the trade-offs between these objectives. Additionally, the inherent simplification associated with formulating a complex multi-objective problem into a weighted single objective problem fails to capture underlying trends. Second, in PV system modelling, most studies use solar irradiation as the only input [18], occasionally combined with temperature [15]. Some studies utilise more accurate PV models which take into account the tilt and azimuth angle of the panel orientations. However, during the design process they select fixed values of tilt and azimuth angle [14], [19] for maximum solar generation. This approach may not result in optimal PV and storage sizes as they do not consider the degree of temporal match of the PV profile and the load profile. Third, many studies do not take into account the effect of load profiles and power management strategy on battery lifetime [11], [13], [17]. Fourth, the impact of incentives given by real-life electricity tariffs on the optimal sizing is not investigated in the literature [14], [15].

The aim of this paper is thus to develop a multi-objective optimisation (MOO) framework to solve the system sizing problem for a grid-connected residential microgrid system to incorporate multiple mutually opposing objectives while taking into account the effect of battery degradation, incentives like feed-in tariffs, and PV system orientation. The developed MOO framework is applied to optimally size the PV-battery-converter system in two residential load profiles in Cabauw, Netherlands (NL), and in Austin, United States (US). The main contributions of this paper compared to previous works are:

Manuscript received March 28, 2019; revised July 1, 2019 and July 26, 2019; accepted August 10, 2019. Date of publication August 19, 2019; date of current version June 19, 2020. This work is part of the research programme P 13-21 with project number A, which is financed by the Netherlands Organisation for Scientific Research (NWO). Paper no. TSTE-00350-2019. *(Corresponding author: Soumya Bandyopadhyay.)*

The authors are with the Department of Electrical Sustainable Energy, DCE&S group, TU Delft, Mekelweg 4, 2628 CD, Delft, The Netherlands (e-mail: s.bandyopadhyay-1@tudelft.nl; G.R.ChandraMouli@tudelft.nl; z.qin-2@tudelft.nl; L.M.RamirezElizondo@tudelft.nl; p.bauer@tudelft.nl).

Color versions of one or more of the figures in this article are available online at http://ieeexplore.ieee.org.

Digital Object Identifier 10.1109/TSTE.2019.2936129

1) Develop a multi-objective optimisation framework to size PV system, grid converter, and battery storage capacity resulting in Pareto fronts of trade-offs between multiple objectives like lifetime capital cost, self-sufficiency, power autonomy and simple payback period.
2) Study the effect of solar meteorological potential on optimal PV and battery sizing by comparing results on two different geographical locations: Cabauw, NL and Austin, US.
3) Investigate the effect of electricity pricing tariffs and feed-in tariffs on optimal sizing of PV and battery system.
4) Draw guidelines for selecting the optimal azimuth angle for a residential PV system.
5) Derive sizing equations and thumb rules to optimally size PV-battery-converter systems for microgrids based on solar potential and specific load profile.

The paper is structured in five parts. In Section II, the techno-economical model of the microgrid is presented. Section III develops the multi-objective optimization (MOO) framework and optimises the sizing of PV-battery based microgrid for two residential load profiles in NL and US. The results of the multi-objective optimisation are presented and analysed in Section IV to derive insights into optimal design and thumb rules for optimal system sizing. Finally, general conclusions are summarised based on the results.

II. Techno-Economical Model of a Microgrid

The techno-economical model of PV-battery based microgrids is presented in this section. The technical model comprises of the PV system model, the battery lifetime model, and the power management strategy. The economic model presents the methodology to compute the lifetime cost which consists of the capital cost and the operational cost. Finally, the figure of merits (FoMs) of a grid-connected PV-battery based residential microgrid are highlighted based on the different metrics produced by the two models.

The technical model is presented in three sub-sections. First, the power and energy output of a rooftop PV system is modelled considering azimuth and tilt angle of the PV panels. Second, the power management strategy to control battery bank power is presented. Finally, the battery lifetime methodology is discussed briefly.

1) PV System Modeling: To estimate the energy and power generated by the rooftop PV array, an accurate PV system model is built in this paper. Based on meteorological data of Netherlands and Texas, US, Global Horizontal Irradiance (S^{GHI}), Diffuse Horizontal Irradiance (S^{DHI}), Direct Normal Irradiance (S^{DNI}) and ambient temperature (T_{a}) are obtained. The PV array is modelled in MATLAB using Sun power E20-327 modules rated at 327 W.

At a certain sun position, the irradiance on a panel with a specific orientation ($A_{\mathrm{m}}, \theta_{\mathrm{m}}$) can be computed using the geometric models and the isotropic sky diffused model:

$$S_{\mathrm{m}}^{\mathrm{DNI}} = S^{\mathrm{DNI}}[\sin\theta_{\mathrm{m}}\cos a_{\mathrm{s}}\cos(A_{\mathrm{m}} - A_{\mathrm{s}}) + \cos\theta_{\mathrm{m}}\sin a_{\mathrm{s}}] \quad (1)$$

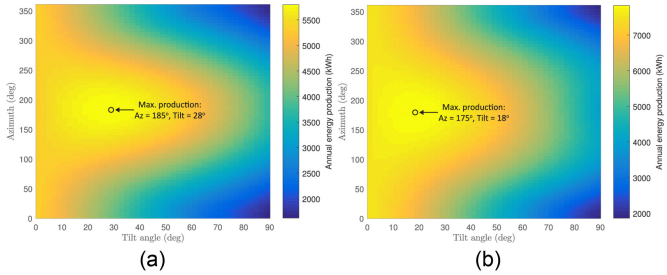

Fig. 1. (a) Annual energy yield of a 5kW PV system in: Cabauw, Netherlands, (b) Annual energy yield of a 5 kW PV system in: Austin, Texas.

$$S_{\mathrm{m}}^{\mathrm{DHI}} = S^{\mathrm{DHI}}\frac{1+\cos\theta_{\mathrm{m}}}{2} \quad (2)$$

$$S_{\mathrm{m}} = S_{\mathrm{m}}^{\mathrm{DNI}} + S_{\mathrm{m}}^{\mathrm{DHI}} \quad (3)$$

where $S_{\mathrm{m}}^{\mathrm{DHI}}$, $S_{\mathrm{m}}^{\mathrm{DNI}}$ are the components of DHI and DNI which are incident on the panel. The above equations show that the solar energy generation by a panel can be controlled by changing the module azimuth (A_{m}) and the tilt angle (θ_{m}).

To improve the PV model accuracy, the effect of the ambient temperature on solar power generation is also taken into consideration. The E20-327 PV module is rated for 327 W at the ambient temperature of 25°. For other ambient temperatures, the PV array output power $P_{\mathrm{solar}}(t)$ at a certain time instant can be computed using [20]:

$$T_{\mathrm{cell}} = T_{\mathrm{a}} + \frac{S_{\mathrm{m}}(T_{\mathrm{NOCT}} - 20)}{800} \quad (4)$$

$$P_{\mathrm{solar}}(t) = \frac{N_{\mathrm{p}}P_{\mathrm{r}}S_{\mathrm{m}}[1-\gamma(T_{\mathrm{cell}} - 25)]}{1000} \quad (5)$$

Fig. 1 shows the annual energy yield for a 5kWp PV array for different azimuth angle and module tilt is estimated for the case of Netherlands (NL) and Texas (TX) based on equations (1)–(5). In case of Netherlands, the maximum annual yield is 5800 kWh obtained for south-facing panels with $A_{\mathrm{m}} = 185°$, $\theta_{\mathrm{m}} = 28°$. The maximum energy yield of 7830 kWh for Austin, Texas is obtained for panels with $A_{\mathrm{m}} = 175°$, $\theta_{\mathrm{m}} = 18°$.

To elaborate the effect of module azimuth orientation, Fig. 2 shows the power output profile of a 5 kW PV system during a summer day in the Netherlands with different azimuth (A_{m}) angles at an optimal tilt angle of $\theta_{\mathrm{m}} = 28°$. By changing the azimuth, the time of the day when maximum PV power is available can be controlled at the cost of lower energy yield. To investigate the effect of module azimuth on optimal storage size sizing, the azimuth angle (A_{m}) is considered as a design variable in the optimisation framework.

2) Power Management Strategy: The goal of the power management strategy is to determine the charging/discharging power of the battery $P_{\mathrm{bess}}(t)$ and grid power $P_{\mathrm{grid}}(t)$ at a certain time instant based on the load power $P_{\mathrm{load}}(t)$ and PV power generation $P_{\mathrm{pv}}(t)$ at that particular instant. Different power management algorithms lead to different solutions to the optimal storage and PV sizing problem. In this study, the state-based power management algorithm approach is considered due to their simplicity, low

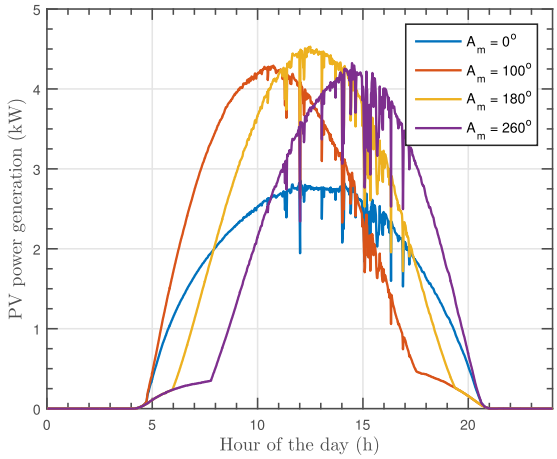

Fig. 2. Power generated by 5 kW PV system for a summer day (Day 165 of year 2017) in Netherlands for different azimuth angles = 0°, 100°, 180°, and 260° with constant tilt angle of 28°.

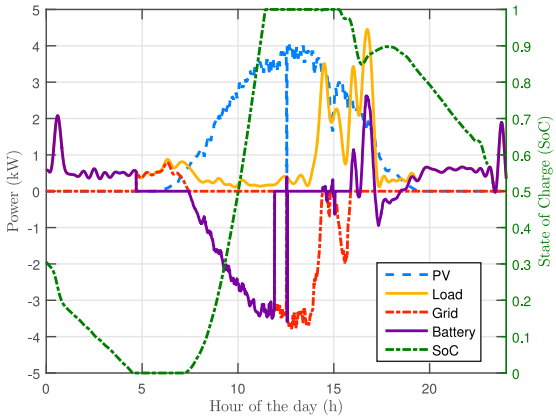

Fig. 3. Power profiles (1 minute resolution) of different sources and overall load along with battery SoC profile on a summer day (day = 240) in Netherlands with battery as primary source algorithm. The simulated house has installed PV power is 5 kW, a lithium ion battery of 10 kWh capacity with C_{rate} of 1 and a 5 kW front-end converter.

computational requirement and ease of real-life implementation. In this algorithm, the battery is used as the primary source all the time. The utility grid is used only on two scenarios: (1) when the battery has reached the minimum allowable SoC, and there is not enough solar generation to provide power to the load, and (2) when the battery has reached the maximum allowable SoC, and the excess solar power is fed into the grid. Fig. 3 shows the power profiles of the grid, battery, PV and load along with the SoC of the battery on a summer day in NL using the algorithm.

3) Battery Lifetime Modelling: In literature, battery ageing is characterised and quantified by the term state of health (SoH). For residential based grid storage application, capacity fading (permanent capacity loss) is used as the primary indicator for SoH of the battery. By convention, in EV batteries, the end-of-life (EOL) condition is reached when the battery capacity has dropped to 80% of its nominal capacity [21]. The same convention is used in this analysis for residential applications. Therefore, the SoH of the battery becomes:

$$\text{SoH} = \left(1 - \frac{\xi}{Q_0}\right).100\% \tag{6}$$

where ξ is the total capacity fade of the battery during operation and Q_0 is the nominal capacity of the battery. It can be seen that when 20% of the nominal battery capacity has faded the SoH of the battery becomes 80% based on (6), and thus the battery system has reached the end-of-life (EOL) condition. The main goal of lifetime modelling process is to estimate the lifetime as a function of the operating conditions associated with the application: $L_{\text{batt}} = f(\text{SoC}, \text{DoD}, C_{\text{tot}})$, where C_{tot} is the total Ah processed by the battery in that load cycle. In this paper, a detailed empirical Li-ion battery lifetime model developed in [22] is used.

This concludes the details of the technical model of the grid-connected microgrid. The economic modelling approach is presented in the next section.

An economic model of the microgrid is required to quantify the benefits of installing a PV and battery system in grid-connected microgrids. The economic benefit comes in form of savings in the electricity bill due to: (a) using PV energy and battery stored energy for houshold loads thereby reducing grid dependency, and (b) selling unused PV power to the grid.

During the system lifetime, the total cost of the system can be divided in two parts: (a) capital cost, and (b) operational costs which include cost of electricity. The cost of battery replacements and maintenance is considered within the capital costs. Thus, the total capital cost (κ_{total}) of a PV-battery integrated grid-connected microgrid can be formulated as the following:

$$\begin{aligned}\kappa_{\text{total}} &= \kappa_{\text{batt}} + \kappa_{\text{pv}} + \kappa_{\text{grid-conv}} \\ &= \pi_{\text{batt}} C_{\text{batt}} (n_{\text{replace}} + 1) + \pi_{\text{pv}} P_{\text{pv,r}} + \pi_{\text{conv}} P_{\text{grid-conv,r}}\end{aligned} \tag{7}$$

where, κ_{Batt}, κ_{pv}, and $\kappa_{\text{grid-conv}}$ are the capital cost associated with the battery storage system, PV system, and the front end grid converter. π_{batt}, π_{pv}, and π_{conv} are unit-price for the battery system, the PV system, and the grid interfacing converter. n_{replace} denotes the number of battery replacements needed during the total system lifetime. Table I shows the values of the constants used in the economic model along with their sources. Next, the electricity tariffs associated with NL and US are discussed in detail.

4) NL Tariff: The electricity tariff in the Netherlands chosen for this study is based on Eneco residential rates [25]. Eneco tariff is based on time-of-use (TOU) prices with peak and off-peak rates as shown in Table II.

TABLE I
OVERVIEW OF ECONOMIC PARAMETERS

Parameter	Symbol	Unit	Value
Converter	π_{conv}	\$/kW	100
PV system [23]	π_{pv}	\$/kWp	1350
Lithium-ion BESS [24]	π_{batt}	\$/kWh	500

TABLE II
NETHERLANDS ENECO ELECTRICITY TARIFFS

Tariff Type	Symbol	Time (hours)	Value (€/kWh)
Peak	c_{p}	9 - 20	0.2202
Off-peak	c_{off}	0-9, 20-24	0.2062
Feed-in	c_{fed}	0-24	0.092

TABLE III
AUSTIN ENERGY ELECTRICITY TARIFF STRUCTURE

Type	Bill Components	Symbol	$/kWh
Administrative Charge	Regulatory charge	c_{rc}	0.013
	Customer charge ($/month)	c_{fixed}	10
Energy charge	Tier 1: 0-500 kWh	$c_{\text{tier,1}}$	0.028
	Tier 2: 501-1000 kWh	$c_{\text{tier,2}}$	0.058
	Tier 3: 1001-1500 kWh	$c_{\text{tier,3}}$	0.078
	Tier 4: 1501-2500 kWh	$c_{\text{tier,4}}$	0.093
	Tier 5: >2500 kWh	$c_{\text{tier,5}}$	0.11
Power supply adjustment	Summer	$c_{\text{psa,s}}$	0.029
	Winter	$c_{\text{psa,w}}$	0.031
Feed-in tariff	Value of Solar (VOS)	c_{fed}	0.097

Based on the data provided, the total electricity bill (κ_{elec}) can be computed based on the following:

$$\kappa_{\text{elec}} = \kappa_{\text{peak}} + \kappa_{\text{off-peak}} \tag{8}$$

$$\begin{aligned}\kappa_{\text{peak}} &= E_{\text{net,p}} c_{\text{p}} \quad \text{if} \quad E_{\text{net,p}} > 0 \\ &= E_{\text{net,p}} c_{\text{fed}} \quad \text{if} \quad E_{\text{net,p}} < 0\end{aligned} \tag{9}$$

$$\begin{aligned}\kappa_{\text{off-peak}} &= E_{\text{net,off}} c_{\text{off}} \quad \text{if} \quad E_{\text{net,off}} > 0 \\ &= E_{\text{net,off}} c_{\text{fed}} \quad \text{if} \quad E_{\text{net,off}} < 0\end{aligned} \tag{10}$$

where $E_{\text{net,i}}$ is the net energy exchanged between the grid and the house for the period i={p,off}:

$$E_{\text{net,i}} = E_{\text{grid-drawn,i}} - E_{\text{grid-fed,i}} \tag{11}$$

5) Texas Tariff: The electricity tariff system for Texas considered in this study is based on Austin energy residential rates [26]. Austin Energy has a five-tier rate structure that incentivises customers on lowering their electric usage resulting in lower bills. Details of the electricity bill are presented in Table III.

Based on the rate structure, the annual electricity bill of a household in Austin, Texas is computed using the following equation:

$$\begin{aligned}\kappa_{\text{elec}} = c_{\text{fixed}} + E_{\text{total}} c_{\text{rc}} + E_{\text{sum}} c_{\text{psa,s}} + E_{\text{win}} c_{\text{psa,w}} \cdots \\ + \sum_{i=1}^{5} E_{\text{tier,i}} c_{\text{tier,i}} - E_{\text{fed}} c_{\text{fed}}\end{aligned} \tag{12}$$

where E_{total} is the total energy exchanged with the grid (drawn and fed), E_{sum} and E_{win} are the energy exchanged with the grid during the summer and the winter months. $E_{\text{tier,i}}$ for i = 1–5 are obtained from the net drawn energy from the grid. E_{fed} is the net energy fed into the grid.

The tariff equation (12) shows that self-consumption by consumers is encouraged as the electricity tariff increases sharply between tiers. Additionally, consumers are encouraged to be producers as well with the Value of Solar (VOS) tariff which Austin Energy credits solar customers for the solar energy produced by their on-site solar energy system. However, it must be noted that the regulatory charge and the power supply adjustment charges discourages consumers to be dependent on the grid in terms of both drawing and feeding in power. In conclusion, multiple objectives like self-consumption or energy autonomy, peak shaving or power autonomy need to be considered while optimally sizing PV and battery system for lowering electricity bill in the Austin Energy tariff structure.

Figure of merits (FoMs) of Microgrids: A detailed description of the modelling methodology of the technical and economic aspects of the PV-battery system integrated microgrid is presented in the previous section. However, to optimally size the PV system, battery storage and the converters, certain performance metrics or figure of merits (FoMs) need to be defined to evaluate and differentiate between designs objectively. To that end, the following four FoMs are introduced.

Energy autonomy factor (α): The grid energy autonomy factor is a metric to measure self-sufficiency or energy independence of the microgrid design. It is calculated as:

$$\gamma = \frac{E_{\text{load}} - E_{\text{grid,buy}}}{E_{\text{load}}} \times 100 \quad (\%) \tag{13}$$

Power autonomy (ρ): Power autonomy factor is a metric to quantify the power independence of the microgrid from the utility grid. It is computed as the following:

$$\rho = \left(1 - \frac{1}{N} \sum_{i=1}^{N} \frac{|P_{\text{grid,i}}|}{|P_{\text{load,i}}|}\right) \times 100 \quad (\%) \tag{14}$$

where N depends on the resolution of the power profiles used. In this study, 1 min resolution is chosen.

Therefore, to compute the power autonomy factor for an annual load profile N is $= 24 \times 60 \times 365$. As the energy autonomy factor (α) measures the energy independence of the microgrid, the power autonomy factor (ρ) measures the power independence which includes both drawn and fed power. For example, the Texas electricity bill as shown in equation (12) incentivises customers to regulate their peak by charging the regulatory and the power supply adjustment costs. However, in Netherlands traiff structure the customer is encouraged to be energy independent and not necessarily power independent.

Lifetime capital cost (κ_{total}): The capital cost of the entire system is an economic metric to quantify the total lifetime cost of the system which includes the initial investment cost, maintenance, and the replacement costs during the system lifetime [27]. Detailed modeling of the capital cost is already shown in equation (7).

Simple payback period (T_{PB}): The simple payback period is a metric to measure the economic viability of the PV-battery based system [23], [28]. It is defined as the number of years needed to pay back the capital cost with the savings related to electricity bill (R_{savings}):

$$T_{\text{PB}}\ (\text{year}) = \frac{\kappa_{\text{total}}}{R_{\text{savings}}} = \frac{\kappa_{\text{total}}}{\kappa_{\text{elec,o}} - \kappa_{\text{elec,pv-batt}}} \tag{15}$$

where $\kappa_{\text{elec,o}}$ and $\kappa_{\text{elec,pv-batt}}$ are the annual electricity bills without and with integrated pv-battery system in the house.

TABLE IV
OPTIMIZATION VARIABLES AND THEIR RANGE

Component	Variable	Symbol	Unit	Variable Range
Battery System	Battery capacity	E_{cap}	kWh	1-30
	C-rate of the battery	C_{rate}	-	0.1-1
	Minimum SoC	SoC_{min}	(%)	0-30
	Depth of discharge	DoD	(%)	20-100
PV System	Azimuth angle	A_{z}	$^{\text{o}}$	100-300
	Rated PV power	$P_{\text{pv,r}}$	kW	0.3-15
Grid converter	Rated power	$P_{\text{grid,r}}$	kW	0-10

The choice of performance metrics is motivated to facilitate both the end-users and the distribution system operators (DSOs). Economic metrics like lifetime system cost and the simple payback period are useful to end-users to analyse the cost-effectiveness of the solutions. On the other hand, fundamental technical metrics like energy autonomy and power autonomy can be utilised by DSOs to design tariff schemes to incentivise users to achieve their higher system-level goals like reducing the operating costs, delay expensive grid upgrades [12], and solving network congestion [29], [30].

This concludes the techno-economical modelling of the PV-battery based microgrid. Based on the model metrics, four FoMs are identified which will be used for the optimisation problem formulation.

III. MULTI-OBJECTIVE OPTIMISATION FRAMEWORK

A multi-objective optimisation framework is developed in this section to optimally size the PV system, the grid converter, and the battery of a microgrid. It utilises the techno-economical model developed in the previous section. Initially, the optimisation targets and variables are described, followed by a discussion on the system analysis flowchart. In the final part of this study, the developed multi-objective optimisation framework is utilised to optimally size the PV-battery for a microgrid in different operational scenarios. The results obtained are presented and analysed in detail in the next section.

A. Optimisation Targets and Variables

Based on the FoMs introduced in the modelling section, the targets of the optimisation are:

1) Maximize energy autonomy factor (α)
2) Maximize power autonomy factor (ρ)
3) Minimize lifetime capital cost (κ_{total})
4) Minimize simple payback period (T_{PB})

The objectives mentioned above are selected strategically to ensure that the optimisation progresses towards designs with acceptable economic and technical performances.

Table IV presents the optimisation variables and their range. The optimisation variables are mainly categorised into three groups: battery variables, PV system variables and the grid converter variables. C_{rate} is chosen as an independent optimisation variable which decides the rated power of the battery $P_{\text{batt,r}}$ based on the battery capacity E_{cap}. To ensure feasible designs, specific constraints are put on the optimisation solution space. In the next part, the multi-objective optimisation algorithm and sizing methodology is discussed in detail.

B. Multi-Objective Optimisation Algorithm and Methodology

Particle swarm optimisation (PSO) algorithm is used for optimising the proposed PV-battery sizing problem. PSO is an evolutionary gradient-free algorithm inspired by the movement of birds or insects in a swarm which potentially requires fewer function calls [31]. However, PSO is a single-objective optimisation algorithm. To make it suitable for multi-objective optimisation problems, the concept of Pareto dominance is combined [32] to generate non-dominated solutions or Pareto-optimal solutions, which results in Pareto fronts. A repository is used to store the Pareto-optimal solutions which are updated at the end of each iteration. Fig. 4 presents the multi-objective optimisation routine in a flowchart depicting the inputs, outputs, and system analysis of the PV-battery optimal sizing problem.

Thirty particles or designs per iteration and two-hundred iterations are evaluated to generate a stable Pareto front between two conflicting objectives. MATLAB is used to compute all the analytical equations presented in the previous section to model the performance parameters or figure of merits (FoMs) of the microgrid design. The time required to evaluate a complete design varies between 15 s–30 s.[1] In this paper, an approach based on placing particles on the border of the search space using a combination of variable clipping and reflecting [31]. The optimisation results for two case studies (Netherlands and US) are discussed in the next section.

IV. OPTIMISATION RESULT ANALYSIS

The MOO framework developed in the previous section is utilised to optimally size the PV-battery-grid converter system in both the Netherlands and the US residential case studies. Fig. 5 shows the real-life load profiles used in this paper. The data for the NL residential load profile is obtained from a Dutch DSO company, and the US profile is obtained from Pecanstreet online database [33]. Table V presents the details regarding the selected household load profiles.

It must be noted that the PV-battery sizing results obtained from the MOO framework for the two case studies are particular solutions for the particular combination of the load profile, solar irradiance profile, battery technology, power management strategy, and electricity tariff structure. Altering any of the above aspects will lead to different conclusions on the PV-battery sizing problem.

The optimisation returns a 4-D Pareto optimal front. To aid visualisation and insight into the results, a detailed analysis is conducted in three steps. First, higher level results are analysed using sub-fronts of two targets. At a second level, complete fronts are shown to aid explanation of underlying trends. Finally, two optimal designs are selected and analysed to verify the efficacy of the optimisation process.

Fig. 6 shows the side views of the 4D Pareto optimal front which highlight the trade-offs between lifetime system cost,

[1] Intel Xeon CPU E5-1620 v2 @ 3.70 GHz, 16 GB RAM.

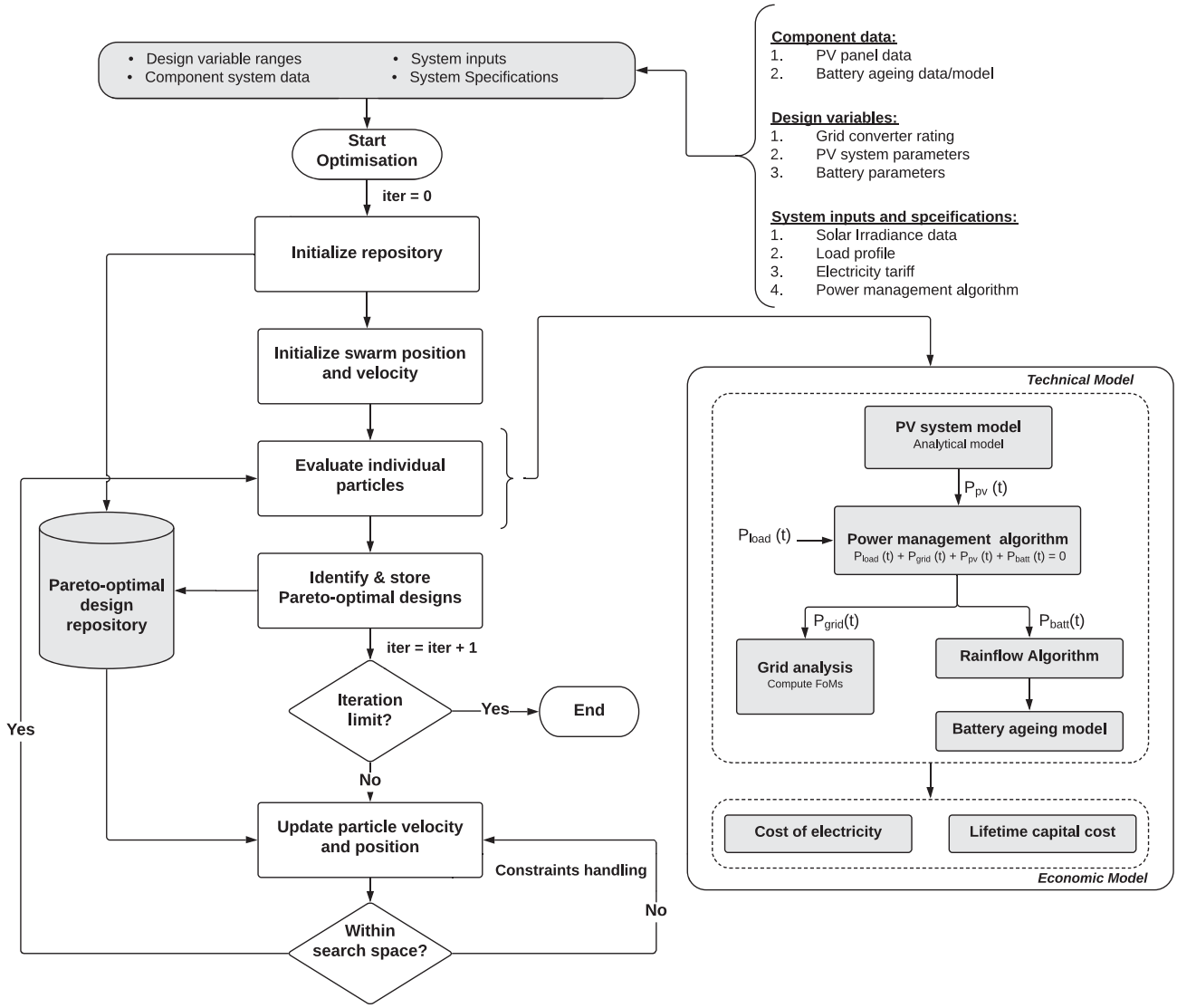

Fig. 4. Flowchart of the proposed main multi-objective optimisation routine for PV-battery sizing for microgrids. The routine calculates and identifies the Pareto-optimal designs as a combination of the optimisation design variables, which include the PV system parameters, battery management parameter, and grid converter ratings. The system analysis for individual designs evaluates the optimisation targets based on the swarm algorithm-generated designs and feeds it back to the optimisation routine to update the Pareto-optimal design repository.

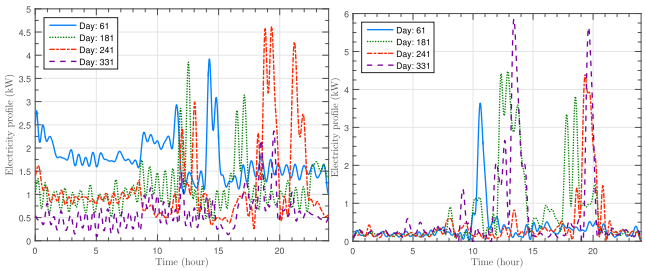

Fig. 5. (a) NL house daily load profile for four days of the year with maximum load $P_{\text{load,max,nl}} = 7$ kW, (b) Texas, US house daily load profile for four days of the year with maximum load $P_{\text{load,max,us}} = 9.8$ kW.

energy autonomy, power autonomy, and payback period. Individual 2D Pareto fronts are discussed in the following:

TABLE V
LOAD PROFILE DETAILS

Description	Symbol	Units	Load profile NL	Load profile US
Energy consumption per day	E_{daily}	kWh	18	17
Peak power annual	$P_{\text{load,max}}$	kW	7	9.8
Annual cost of electricity	$\kappa_{\text{elec,o}}$	$	1630	840

A. Pareto Front Analysis

$\alpha - \kappa_{total}$ *Pareto front:* In the case of Texas load profile, it is evident from the fronts shown in Fig. 6, that full energy autonomy is achievable after significant capital investment. However, in the case of the NL residential profile, it is difficult to achieve full energy autonomy, which asymptotes around 70%. It can be explained due to the low solar potential combined with the temporal mismatch between the yearly solar generation

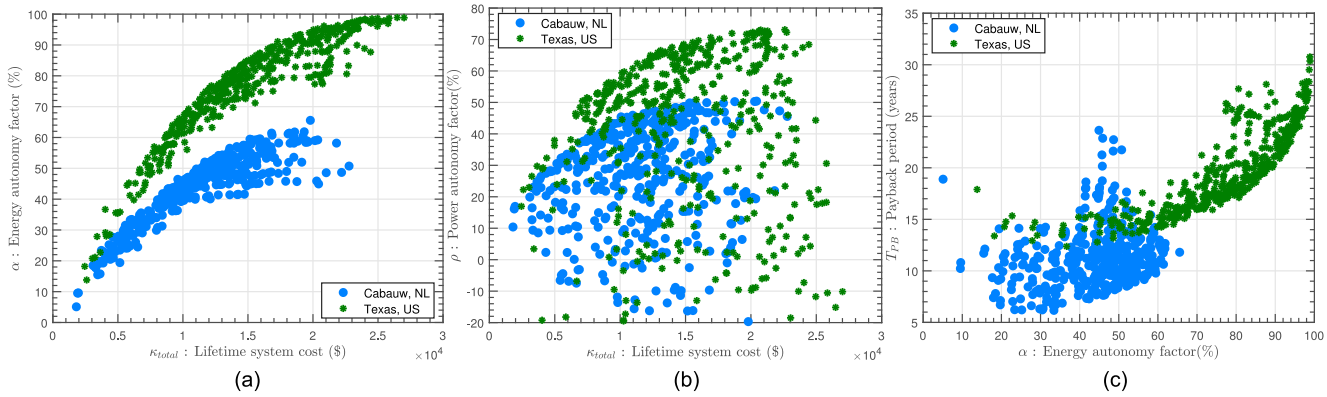

Fig. 6. Results of multi-objective optimisation for PV-battery sizing with NL and US houseload profile: (a) $\alpha - \kappa_{\text{total}}$: Pareto fronts of trade off between energy autonomy factor and lifetime system cost, (b) $\rho - \kappa_{\text{total}}$: Pareto fronts of trade off between power autonomy and lifetime system cost, and (c) $T_{\text{PB}} - \kappa_{\text{total}}$: Pareto-fronts of simple payback period and power autonomy factor.

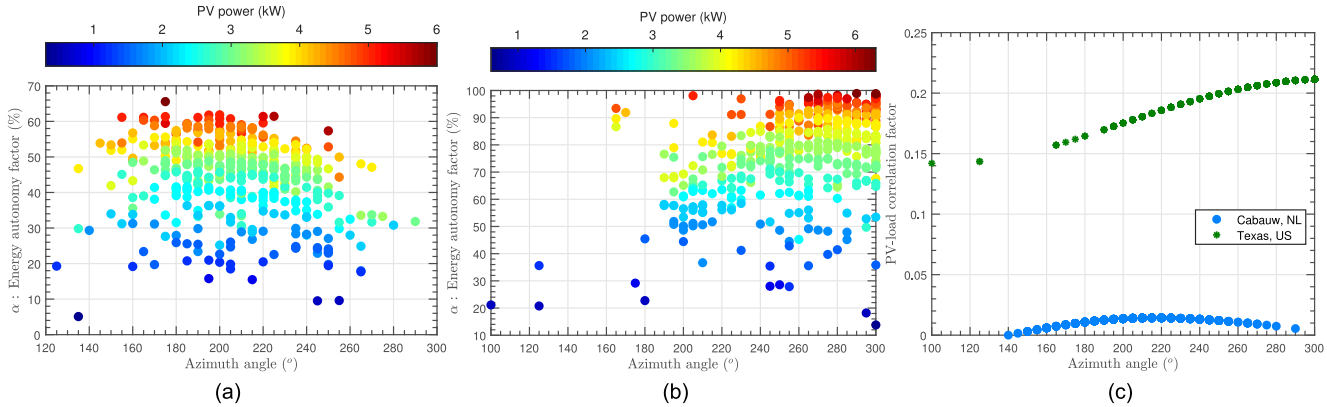

Fig. 7. Effect of PV module azimuth angle on: (a) energy autonomy for different PV power for Cabauw, NL, (b) energy autonomy for different PV power for Texas, US, (c) correlation coefficient between annual pv generation profile and load profile for the case of NL and US.

profile (Fig. 10a) and daily energy usage profile (Fig. 10b) of the Netherlands. Therefore, to achieve full energy autonomy in case of NL load profiles, battery-based storage is not sufficient and seasonal storage is required.

$\rho - \kappa_{total}$ *Pareto front:* Fig. 6b shows that full power autonomy is hard to achieve in both NL and US case studies with maximum possible values of 50% and 70% respectively. Additionally, it is evident that power autonomy can be negative in certain cases. Negative power autonomy is due to feeding more power into the grid compared to the actual in-house load power demand which leads to even lower electric bills.

$T_{PB} - \alpha$ *Pareto front:* The trade-off between simple payback period and energy autonomy is presented in Fig. 6c. Previously it is shown that the US-based PV-battery system performs much better than the NL system in terms of both power autonomy and energy autonomy for the same capital investment. However, the NL based PV-battery system performs significantly better in the metric of simple payback period (T_{PB}) for certain energy autonomy. It can be explained due to the following reasons: (a) the annual electricity bill for the NL load profile without any PV and battery is 1630 $ compared to 840 $ in case of the US Austin load profile leading to higher the savings potential for the NL case is much higher and therefore leads to lower payback period, and (b) the NL electricity tariff heavily incentivises the end-user to be energy autonomous by installing PV with battery storage compared to the Austin tariff. This result underlines the importance of incorporating the cost of electricity model in the optimisation problem.

B. PV-battery System Design and Sizing Trends

Underlying trends regarding the battery system design, PV system design and sizing are analysed in this section. Fig. 8 presents the maximum allowable depth of discharge (DoD) of the Li-ion battery system of the optimised designs. The maximum allowable DoD of the Li-ion battery system increases with the increase of the battery capacity for both NL and US. Based on that, it is concluded that for optimal performance of a Li-ion based microgrid, one should select a proper DoD range depending on the size of the battery. For these particular case studies, a smaller capacity battery ($\leq$5 kWh) has an optimal maximum DoD of 40%–70%. The optimal maximum DoD

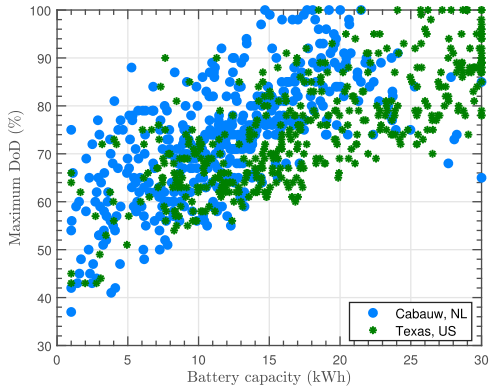

Fig. 8. Maximum allowable DoD vs. the battery capacity of the optimal Pareto system designs.

is 65%–90% for battery capacities ranging from 10 kWh to 20 kWh. 100% DoD of the battery can be utilised for battery sizes bigger than 20 kWh when the capacity fading due to daily cycles is insignificant compared to the nominal battery capacity for this particular application.

In Section II-1, the potential of changing the azimuth angle A_{m} to improve the temporal match between the pv generation profile and the houseload profile was presented. To that end, A_z was considered to be a design variable in the optimisation framework (Table IV). Fig. 7a and 7b presents the range of A_{m} for the optimal designs for the NL and US case studies respectively. In case of the NL designs the optimal range is between 180°–220° whereas for the case of Austin, US the optimal range is 240°–300°. It is interesting to highlight that the optimal designs have significantly different A_{m} from the maximum energy generation $A_{\mathrm{m,max}}$ which is 185° for NL and 175° for the US case (Fig. 1). To explain this result, a new metric based on the Pearson correlation coefficient is defined to quantify the temporal match between the PV power profile and load profile:

$$\gamma(P_{\mathrm{pv}}, P_{\mathrm{load}}) = \frac{1}{N-1}\sum_{i=1}^{N}\left(\frac{P_{\mathrm{pv,i}}-\mu_{\mathrm{pv}}}{\sigma_{\mathrm{pv}}}\right)\left(\frac{P_{\mathrm{load,i}}-\mu_{\mathrm{load}}}{\sigma_{\mathrm{load}}}\right) \tag{16}$$

where P_{j}, μ_{j}, and σ_{j} are the annual power profile, mean and the standard deviation of the power profile for the jth system with $\mathrm{j} = \{\mathrm{pv}, \mathrm{load}\}$. The correlation co-efficient γ represents the degree of temporal match between the PV profile and the load profile. γ ranges from 1 (complete temporal match) to -1 (complete temporal mismatch). Fig. 7c shows the variation of correlation coefficient γ with the choice of azimuth angle for both the NL and the US case studies. It is evident from Fig. 7, that the optimal choice of azimuth angle A_{m} for pv-battery system design is the one which results in maximum temporal match between the pv profile and the load profile. Additionally, the correlation coefficient γ for the case of NL load profile and PV profile is almost 10 times lower compared to the case of the US profile. It is expected since there is significant mismatch between the annual solar profile and load profile for the NL case study. Fig. 10a and Fig. 10b show that there is high load demand and low solar generation during winter coupled with comparatively lower load demand and higher solar generation during the summer. However, in the US case study, the seasonal load demand variations match the seasonal PV profile variations leading to high values of correlation coefficient γ.

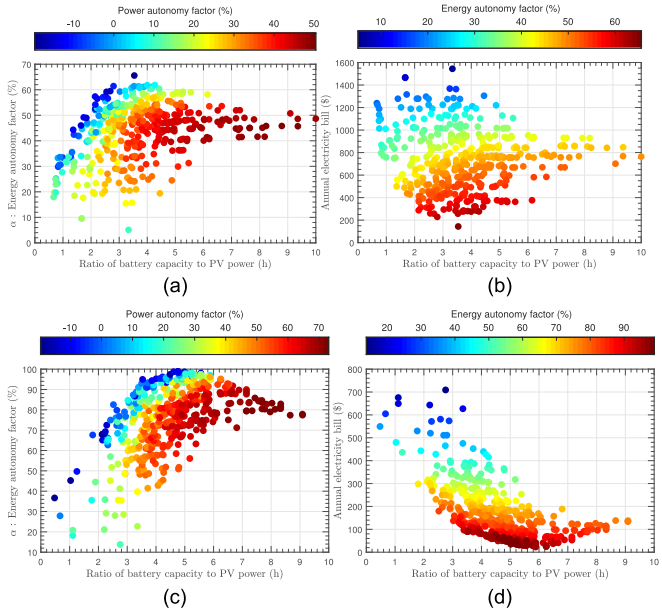

Fig. 9. Results of multi-objective optimisation for PV-battery sizing with NL and US houseload profile: (a) variation of energy autonomy factor with storage hours (S_{h}) or ratio of battery capacity to rated pv power in case of NL, (b) variation of annual cost of electricity with S_{h} in case of NL and (c) variation of energy autonomy factor with S_{h} in case of US, (d) variation of annual cost of electricity with S_{h} in case of US.

Finally, it is important to derive design thumb rules to select PV system size and battery capacity to achieve optimal performance for a certain capital investment. In this considered PV-battery system for grid-connected microgrids there are four unknown variables: $P_{\mathrm{pv,r}}$, $P_{\mathrm{batt,r}}$, $P_{\mathrm{grid,r}}$, and E_{cap}. For the relative sizing of PV power and battery capacity, a metric called storage hours (S_{h}) is defined as following:

$$S_{\mathrm{h}} = \frac{E_{\mathrm{cap}}}{P_{\mathrm{pv,r}}} \tag{17}$$

Fig. 9a shows the effect of storage hours on the energy autonomy of the PV-battery based microgrid for the NL case study. It can be seen that the optimal range of S_{h} is 2 to 4 which also results in the minimum annual cost of electricity as shown in Fig. 9b. Applying similar analysis to the case of US as shown in Fig. 9c and 9d, the optimal range of S_{h} turns out to be 4 to 6. Since Texas, US has higher solar potential (≈35%) compared to Cabauw, NL, it is intuitive that a bigger sized battery is needed to properly harness the excess solar potential. This ratio can be used as a thumb rule for sizing PV and battery system for a microgrid in Netherlands and US, Texas to ensure high performance for a fixed capital cost.

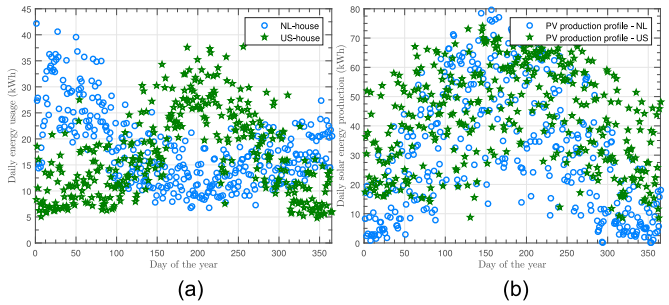

Fig. 10. (a) Annual daily energy usage profile for the NL with a daily average of 18 kWh and US load profile with a daily average of 17 kWh, (b) comparison of solar energy production throughout the year in Cabauw, Netherlands and Austin, Texas for a 5 kW PV system designed for maximum annual solar output.

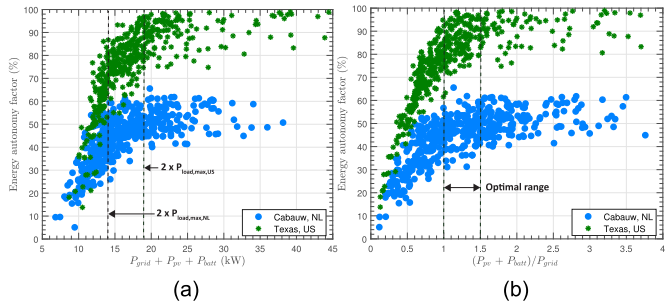

Fig. 11. Variation of energy autonomy factor with (a) sum of all the source converter ratings $P_{\text{sum,total}}$, (b) ratio of the sum of PV-battery converter ratings to the grid converter rating P_{ratio}.

To optimally size the different converters associated with the grid, PV, and the storage, two additional metrics or equations are introduced:

$$P_{\text{sum,total}} = P_{\text{grid,r}} + P_{\text{pv,r}} + P_{\text{batt,r}} \tag{18}$$

$$P_{\text{ratio}} = \frac{(P_{\text{pv,r}} + P_{\text{batt,r}})}{P_{\text{grid,r}}} \tag{19}$$

where $P_{\text{sum,total}}$ represents the sum of all the source/storage converter ratings, and P_{ratio} is the ratio of the sum of PV-battery converters to the grid converter rating. Fig. 11 presents the effect of the two aforementioned metrics on the energy autonomy of the microgrid optimal designs for both the case studies. In case of the NL house, a $P_{\text{sum,total}}$ of 15 kW or above will result in high energy autonomy. Similarly a $P_{\text{sum,total}}$ of 20 kW or above is required for high energy autonomy for the Austin, US house. It is interesting to point out that the maximum load power in case of NL and US are 7 kW and 9.8 kW respectively which are approximately half of the thresholds required for high energy autonomy. Similarly, from analysing Fig. 11b, the optimal converter ratio factor P_{ratio} lies somewhere around 1–1.5 for both the case studies of NL and US. As for sizing guidelines, one can select a certain rated power for the PV system depending on the avaliable area for PV installation and use equations (17), (18), (19) as thumb rules to optimally size the battery capacity, and the converter sizes for a grid connected microgrid. Table VI summarizes all the sizing equations derived from analyzing the data obtained from the optimisation procedure.

TABLE VI
SYSTEM SIZING THUMB RULES

Sizing equation	Cabauw, NL	Austin, US
S_{h}	2 - 4	4 - 6
$P_{\text{grid,r}} + P_{\text{pv,r}} + P_{\text{batt,r}}$	$\geq 2P_{\text{load,max}}$	$\geq 2P_{\text{load,max}}$
$\frac{(P_{\text{pv,r}} + P_{\text{batt,r}})}{P_{\text{grid,r}}}$	1 - 1.5	1 - 1.5

C. Analysis of Selected Optimal Designs

Higher level design sizing trends are obtained in the previous section by analysing the optimisation results. To highlight the efficacy of the sizing optimisation procedure, we have selected two Pareto optimal microgrid designs for more in-depth analysis. The designs are chosen with the same total lifetime cost of 13,000 $ to ensure a fair comparison.

Table VII presents the important design and performance metrics of the two selected design cases. In terms of pv-battery system sizing, the NL microgrid has a higher power PV system and lower battery capacity compared to the US counterpart. Due to higher solar potential, the US microgrid needs a slightly bigger battery to store the excess solar energy. Both the microgrid designs under-utilise the battery capacity by selecting a maximum allowable DoD of 63% (NL) and 70% (US) to extend the lithium-ion battery lifetime.

In performance factors like energy autonomy and power autonomy, the NL microgrid lags behind the US microgrid. Still, the NL microgrid performs much better economically with simple payback period almost half that of the US microgrid design. This is mainly due to two reasons. First, the annual cost of electricity for the US house is significantly lower than the NL house (see Table V) for almost similar energy consumption, thereby limiting the savings margin. Second, the Dutch electricity provider incentivises high energy autonomy with net-metering based tariff system, whereas the US tariff system incentivises high power autonomy, which is a comparatively more difficult metric to achieve. Fig. 12 presents the annual grid power profiles of the two selected case studies. It is evident from the profile (Fig. 12a) that the NL house microgrid interacts heavily with the utility grid throughout the year, which results in weak power autonomy of 15%. During winter, when the solar generation is low, and the load requirement is high, it depends solely on the grid to supply the load. However, during the summer days when the load is comparatively lighter, and solar power is higher, the microgrid consistently dumps the excess solar energy to the utility grid. Therefore, the NL microgrid is highly energy-positive during the winter days and highly energy-negative during the summer days, which eventually balances out due to the electricity tariff's sole dependence on energy autonomy rather than power autonomy. This leads to low simple payback period for the NL microgrid. However, unlike the NL microgrid, the US microgrid has weaker interaction with the grid as the Texas electricity tariff incentivises power autonomy,

TABLE VII
RESULTS OF SELECTED OPTIMISED MICROGRID DESIGNS

Performance Group	Performance Metrics	Symbol	Unit	Cabauw, NL	Texas, US
Design parameters	Rated PV power	$P_{\text{pv,r}}$	kW	4.2	3.3
	Battery capacity	E_{cap}	kWh	13	15
	Battery rated power	$P_{\text{batt,r}}$	kW	3.8	4.8
	Grid converter rating	$P_{\text{grid,r}}$	kW	5.6	8.1
	Azimuth angle	A_{m}	^{o}	205	250
	Battery DoD max	DoD	%	63	70
Sizing parameters	Storage hours	S_{h}	h	3.1	4.5
	Total converter ratings	$P_{\text{sum,total}}$	kW	13.6	16.2
	Converter ratings ratio	P_{ratio}	-	1.4	1
Microgrid Performance	Energy autonomy	α	%	54	74
	Power autonomy	ρ	%	15	57
	Payback period	T_{PB}	years	11	20
	Electricity bill	κ_{elec}	$	436	178
	PV Cost	κ_{pv}	$	5460	4290
	Battery cost	κ_{batt}	$	6520	7400
	Total lifetime cost	κ_{total}	$	13000	13000

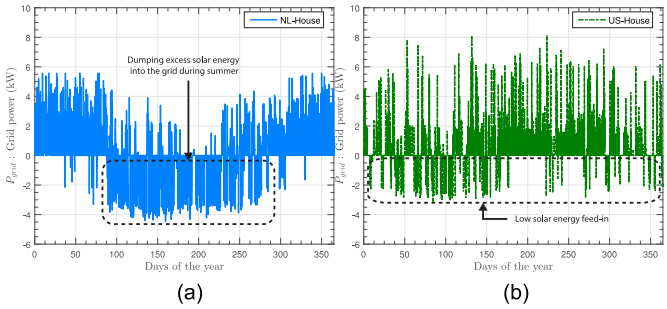

Fig. 12. Annual profile of the power exchange of microgrids with the utility grid (P_{grid}): (a) NL house microgrid, (b) US house microgrid.

which leads to less dumping of solar power in the grid. Therefore, it is economically more viable to install PV and battery system for the NL case study compared to the US case study although the solar potential of Texas, US is much higher than Cabauw, NL.

V. CONCLUSION

This paper presents a multi-objective optimisation (MOO) procedure to size the PV-battery-converter system for microgrid applications. To validate the advantages of the proposed method, the MOO framework is applied to optimally size PV-lithium-ion (Li-ion) battery-converter system for two residential case studies in Cabauw, Netherlands and Austin, US. An in-depth microgrid model considering battery degradation, PV design variables, and real-life electricity tariffs are coupled with the MOO framework with the goal of drawing design guidelines for optimal system sizing. Some essential observations obtained from a detailed analysis of the optimisation results are presented below:

1) The local electricity tariffs in Cabauw, NL heavily incentivises energy autonomy with significant feed-in tariffs leading to low payback periods for an initial investment. However, Austin electricity tariffs incentivise power autonomy by power-based tariffs, which lead to higher payback periods for an initial investment.
2) Solar potential of a location has a significant impact on the relative sizing of the battery capacity relative to the rated PV power. The optimal value of storage hour ($S_{\text{h}} = \frac{E_{\text{cap}}}{P_{\text{pv,r}}}$) for Cabauw is between 2 to 4, whereas for Austin it is between 4 to 6.
3) Optimal value of the azimuth angle (A_{m}) for the PV system is found to be the one which results in a maximum temporal match between the annual PV and load profile.
4) Thumb rules for optimal system sizing are derived to size the battery power rating, battery capacity, PV power rating, and the grid converter rating in equations in Table VI for grid-connected microgrid application.

In conclusion, the presented multi-objective optimisation process provides a platform to optimally size PV-battery systems during the initial design process taking into account a multitude of design variables and multiple objectives. For future work, this study can be extended to compare different battery technologies to select the most economical design. Additionally, the effect of intelligent power management algorithms with forecasting capability on the system sizing problem can be investigated with this framework.

ACKNOWLEDGMENT

The authors would like to thank Netherlands Organisation for Scientific Research (NWO) for providing funding for this research.

REFERENCES

[1] L. Pérez-Lombard, J. Ortiz, and C. Pout, "A review on buildings energy consumption information," *Energy Buildings*, 2008.
[2] A. Dubey and S. Santoso, "Electric vehicle charging on residential distribution systems: Impacts and mitigations," *IEEE Access*, vol. 3, 2015.
[3] E. Veldman, M. Gibescu, H. Slootweg, and W. L. Kling, "Impact of electrification of residential heating on loading of distribution networks," in *PowerTech, 2011 IEEE Trondheim*, pp. 1–7, 2011.
[4] A. Peacock and M. Newborough, "Controlling micro-CHP systems to modulate electrical load profiles," *Energy*, 2007.
[5] D. Kumar, F. Zare, and A. Ghosh, "DC microgrid technology: System architectures, AC grid interfaces, grounding schemes, power quality, communication networks, applications, and standardizations aspects," *IEEE Access*, vol. 5, pp. 12230–12256, 2017.

[6] V. Vossos, K. Garbesi, and H. Shen, "Energy savings from direct-dc in US residential buildings," *Energy Buildings*, 2014.
[7] T.-F. Wu, Y.-K. Chen, G.-R. Yu, and Y. Chang, "Design and development of dc-distributed system with grid connection for residential applications," in *Proc. IEEE 8th Int. Conf. Power Electron. ECCE Asia (ICPE & ECCE)*, IEEE, 2011, pp. 235–241.
[8] U. Boeke and M. Wendt, "DC power grids for buildings," in *Proc. IEEE 1st Int. Conf. DC Microgrids (ICDCM)*, IEEE, 2015, pp. 210–214.
[9] E. Rodriguez-Diaz, J. C. Vasquez, and J. M. Guerrero, "Potential energy savings by using direct current for residential applications: A Danish household study case," in *Proc. IEEE 2nd Int. Conf. DC Microgrids (ICDCM)*, IEEE, 2017, pp. 547–552.
[10] T. Beck, H. Kondziella, G. Huard, and T. Bruckner, "Assessing the influence of the temporal resolution of electrical load and PV generation profiles on self-consumption and sizing of PV-battery systems," *Appl. Energy*, vol. 173, pp. 331–342, 2016.
[11] E. Tervo, K. Agbim, F. DeAngelis, J. Hernandez, H. K. Kim, and A. Odukomaiya, "An economic analysis of residential photovoltaic systems with lithium ion battery storage in the United States," *Renewable Sustain. Energy Rev.*, vol. 94, pp. 1057–1066, 2018.
[12] J. Tant, F. Geth, D. Six, P. Tant, and J. Driesen, "Multiobjective battery storage to improve PV integration in residential distribution grids," *IEEE Trans. Sustain. Energy*, vol. 4, no. 1, pp. 182–191, 2013.
[13] W. L. Schram, I. Lampropoulos, and W. G. van Sark, "Photovoltaic systems coupled with batteries that are optimally sized for household self-consumption: Assessment of peak shaving potential," *Appl. Energy*, vol. 223, pp. 69–81, 2018.
[14] J. Moshövel *et al.*, "Analysis of the maximal possible grid relief from PV-peak-power impacts by using storage systems for increased self-consumption," *Appl. Energy*, 2015.
[15] R. Atia and N. Yamada, "Sizing and analysis of renewable energy and battery systems in residential microgrids," *IEEE Trans. Smart Grid*, vol. 7, no. 3, pp. 1204–1213, 2016.
[16] T. Dragičević, H. Pandžić, D. Škrlec, I. Kuzle, J. M. Guerrero, and D. S. Kirschen, "Capacity optimization of renewable energy sources and battery storage in an autonomous telecommunication facility," *IEEE Trans. Sustain. Energy*, 2014.
[17] S. Kahrobaee, S. Asgarpoor, and W. Qiao, "Optimum sizing of distributed generation and storage capacity in smart households," *IEEE Trans. Smart Grid*, vol. 4, no. 4, pp. 1791–1801, 2013.
[18] M. Bortolini, M. Gamberi, and A. Graziani, "Technical and economic design of photovoltaic and battery energy storage system," *Energy Convers. Manag.*, vol. 86, pp. 81–92, 2014.
[19] L. Xu, X. Ruan, C. Mao, B. Zhang, and Y. Luo, "An improved optimal sizing method for wind-solar-battery hybrid power system," *IEEE Trans. Sustain. Energy*, vol. 4, no. 3, 2013.
[20] G. C. Mouli, P. Bauer, and M. Zeman, "System design for a solar powered electric vehicle charging station for workplaces," *Appl. Energy*, vol. 168, 2016.
[21] M. O. Ramoni and H.-C. Zhang, "End-of-life (eol) issues and options for electric vehicle batteries," *Clean Technol. Environmental Policy*, vol. 15, no. 6, pp. 881–891, 2013.
[22] L. Lam and P. Bauer, "Practical capacity fading model for Li-ion battery cells in electric vehicles," *IEEE Trans. Power Electron.*, vol. 28, no. 12, pp. 5910–5918, Dec. 2013.
[23] C. N. Truong, M. Naumann, R. C. Karl, M. Müller, A. Jossen, and H. C. Hesse, "Economics of residential photovoltaic battery systems in germany: The case of teslas powerwall," *Batteries*, 2016.
[24] D. Akinyele, J. Belikov, and Y. Levron, "Battery storage technologies for electrical applications: Impact in stand-alone photovoltaic systems," *Energies*, vol. 10, no. 11, p. 1760, 2017.
[25] Eneco, "Residential electricity tariffs netherlands," 2017. [Online]. Available: https://www.eneco.nl/zonnepanelen/saldering/
[26] A. Energy, "Residential electricity tariffs texas," [Online]. Available: https://austinenergy.com/ae/residential/rates
[27] B. Zakeri and S. Syri, "Electrical energy storage systems: A comparative life cycle cost analysis," *Renewable Sustain. Energy Rev.*, vol. 42, pp. 569–596, 2015.
[28] J. Li, Z. Wu, S. Zhou, H. Fu, and X.-P. Zhang, "Aggregator service for pv and battery energy storage systems of residential building," *CSEE J. Power Energy Syst.*, vol. 1, no. 4, pp. 3–11, 2015.
[29] F. Shen, S. Huang, Q. Wu, S. Repo, Y. Xu, and J. Østergaard, "Comprehensive congestion management for distribution networks based on dynamic tariff, reconfiguration and re-profiling product," *IEEE Trans. Smart Grid*, vol. 10, no. 5, pp. 4795–4805, Sep. 2019.
[30] J. H. Yoon, R. Baldick, and A. Novoselac, "Dynamic demand response controller based on real-time retail price for residential buildings," *IEEE Trans. Smart Grid*, vol. 5, no. 1, pp. 121–129, Jan. 2014.
[31] Y. Del Valle, G. K. Venayagamoorthy, S. Mohagheghi, J.-C. Hernandez, and R. G. Harley, "Particle swarm optimization: Basic concepts, variants and applications in power systems," *IEEE Trans. Evol. Comput.*, vol. 12, no. 2, pp. 171–195, Mar. 2008.
[32] C. A. C. Coello *et al.*, *Evolutionary Algorithms for Solving Multi-objective Problems*. Springer, 2007.
[33] P. Street, "Pecan street online database," Pecan Street: Austin, TX, USA, 2016.

Soumya Bandyopadhyay received the B.Tech. degree (Hons.) in electrical and electronics engineering from Jadavpur University, Kolkata, India, in 2011 and the M.Sc. degree in electrical engineering in 2015 from the Delft University of Technology, Delft, The Netherlands. Since 2016, he has been working toward the PhD degree in of key power electronics in low voltage dc distribution systems. His research interests include multi-port dc-dc converter design for renewable sources and storages, smart charging of electric vehicles, and wireless power transfer.

Gautham Ram Chandra Mouli received the bachelor's degree in electrical engineering from the National Institute of Technology Trichy, Tiruchirappalli, India, in 2011, and the master's degree in electrical engineering from the the Delft University of Technology, Delft, The Netherlands, in 2013, and the Ph.D. degree from the Delft University, Delft, The Netherlands, in 2018, for the development of a solar powered V2G electric vehicle charger compatible with CHAdeMO, CCS/COMBO and designed smart charging algorithms. He is currently an Assistant Professor with the Department of Electrical Sustainable Energy, Delft University of Technology, Delft, The Netherlands. The project was in collaboration with PRE Power Developers, ABB, and UT Austin. His current research focuses on electric vehicles, EV charging, PV systems, power electronics, and demand-side management. He was awarded the Most Significant Innovation in electric vehicles at the IDTechEx Show 2018 and the Best Tech Idea of 2018 by KIJK. From 2017 to 2019, he was a Postdoctoral Researcher with TU Delft, working on Flexgrid, Trolley 2.0, and Orchestrating Smart Charging in mass Deployment project.

Zian Qin (M'15) received the B.E. degree in automation from Beihang University, Beijing, China, in 2009, the M.E. degree in control science and engineering from the Beijing Institute of Technology, Beijing, China, in 2012, and the Ph.D. degree in power electronics from Aalborg University, Aalborg, Denmark, in 2015. He is currently an Assistant Professor with the Delft University of Technology, Delft, Netherlands. He was a Visiting Scientist with the Institute for Power Generation and Storage Systems (PGS), Aachen University, Aachen, Germany, from April to July 2014. From August 2015 to June 2017, he was a Postdoctoral Research Fellow with Aalborg University.

He is a member of IEEE Power Electronics Society, IEEE Industrial Electronics Society, and IEEE Industry Application Society. His current research interests include application of wide bandgap devices, high frequency power electronics, modelling, control and stability of grid-tied power electronics, energy storage and battery management systems, renewable energy technologies, DC technologies.

Laura Ramirez Elizondo (M'06) was born in San Jos, Costa Rica. She received the bachelor's degree in electrical engineering from the Universidad de Costa Rica in 2003 and the M.Sc. degree (Hons.) in electrical power systems from the Delft University of Technology, The Netherlands, in 2007. From September 2007 to December 2011, she worked on her Ph.D. project.

She is currently an Assistant Professor with the DC Systems, Energy Conversion & Storage group. She is involved in the projects STW Perspektief P13-21: Smart Energy Management and Services in Buildings and Grids (SES-BE), KI Switch 2 Smart Grids: Flexible and future power links for smart grids (FLINK), and NWO URSES project: Gaming beyond the Copper Plate. Her research interests include integration of renewable sources, direct current networks, microgrids, optimization, and power control. In 2013, she was awarded with the Erasmus Energy Science Award.

Pavol Bauer (SM'07) received the master's degree in electrical engineering from the Technical University of Kosice, Kosice, Slovakia, in 1985, and the Ph.D. degree from the Delft University of Technology, Delft, The Netherlands, in 1995.

He is currently a Full Professor with the Department of Electrical Sustainable Energy, Delft University of Technology, and the Head of DC Systems, Energy Conversion and Storage Group. From 2002 to 2003, he was working partially with KEMA (DNV GL, Arnhem) on different projects related to power electronics applications in power systems. He authored or coauthored more than 95 journal and more than 300 conference papers in his field (with H factor Google scholar 35, Web of science 23). He is an author or coauthor of eight books, holds four international patents, and organized several tutorials at the international conferences. He has worked on many projects for industry concerning wind and wave energy, power electronic applications for power systems such as Smarttrafo; HVDC systems, projects for smart cities such as photovoltaic (PV) charging of electric vehicles, PV and storage integration, contactless charging; and he participated in several Leonardo da Vinci and H2020 EU projects as a Project Partner (ELINA, INETELE, E-Pragmatic) and a Coordinator (PEMCWebLab.com-Edipe, SustEner, Eranet DCMICRO).

Dr. Bauer is the Former Chairman of Benelux IEEE Joint Industry Applications Society, Power Electronics and Power Engineering Society Chapter, the Chairman of the Power Electronics and Motion Control Council, a member of the Executive Committee of European Power Electronics Association, and also a member of the International Steering Committee at numerous conferences. He was a recipient of the title Professor from the President of Czech Republic at the Brno University of Technology, Brno, Czech Republic, in 2008, and the Delft University of Technology, in 2016.